THEORY AND ALGORITHMS OF DSM GENERATION FROM MULTI-LINE-ARRAY IMAGES MATCHING

LeiRong*，Fan Dazhao，Ji Song，Zhai Huiqin

Zhengzhou Institute of Surveying and Mapping, Zhengzhou, 450052, China - leirong@163.com

Commission VI, WG VI/5

KEY WORDS: Multi-line-array digital images, DSM; CCD; ADS40; Correlative Coefficient; POS

ABSTRACT:

A new multiple images matching theory model is proposed in this paper to generate DSM from aerial three line array digital images. Through this model, multiple images (more than 2) can be matched simultaneously and the epipolar line constraint can be used indirectly. Theoretically, the occlusion and multiple solution problems, which are unavoidable in traditionally image matching process, can be greatly solved by this model. Based on the robust multi-image matching algorithms, intelligent DSM generation procedure is constructed, and some key techniques during the DSM generation process are investigated. Experiments prove that the DSM generation methods proposed in this paper can effectively generate reliable DSM form multi-line-array digital images.. At the end of this paper, problems remaining to be studied are presented.

1. INTRODUCTION

With the development of sensors and their application technique since 1990s, it will not take a long time for film cameras to be replaced by CCD digital cameras.，which is one of the most significant developing trends of aerial photogrammetry. Now there are two developing trends for CCD digital camera, one is big plane array and another is linear array. Currently, plane array CCD doesn't have enough pixels to meet the requirements of practical photogrammetric applications. To solve this problem, one way is combining a few plane array CCD to produce a big one, but it is expensive and brings the other problems in the real-time transferring and storing of massive changing data. Additionally, some arrays of plane array CCD are randomly distributed, which will result in the losing of image pixels and the bringing of more parameters for geometric and radiometric correction than linear array CCD. Thereby, under the existing research condition, linear array CCD digital cameras are the optimal choice for aerial photogrammetry. At present, some leading experimental and commercial digital camera such as WAOSS, MOMS, WAAC, DPA, ADS40, TLS and JAS and so on are all three line array CCD digital cameras. Among these digital camera systems, ADS40 is the first commercial airborne three line array digital camera system developed by Leica Company and the DLR institution.

Digital Surface Model (DSM) is often referred to as the model for the first reflective or visible surface. DSM is an vital product of digital photogrammetry and plays an irreplaceable role in such aspects as determining objects' height, generating DEM, producing true ortho-image, automatic recognizing and extracting buildings and so on. Recently, the techniques of digital sensor have undergone a significant development and many sensor systems can obtain multiple images of the same area simultaneously. As an example, for ADS40, there are 3 to 7 highly overlapping images on the same flight strip (the overlapping degree of neighboring images is nearly 90%) for any imaging area. Moreover, the ADS40's overlapping degree of neighboring flight strip is around 60% and this provides more images for the imaging area. The high overlapping images provides redundant information for automatic DSM generation. However, it is quite complex to generate DSM form three line array digital images and multiple image matching technique is one bottleneck. To generate dense and precise DSM, such problems as image occlusion, multiple solution, noise, surface discontinuity and so on have to be solved effectively, which requires new image processing techniques.

2. MULTI-IMAGE MATCHING ALGORITHM MODEL

As is shown in Figure 1, consider three ADS40 digital images, which are obtained on the same flight line. I0, I1 and I2 are nadir, forward and backward image respectively, where I0 is selected as reference image, and Ii (i=1, 2) are selected as searching images.The basic working process of AMMGC model can be described as follows.

(1) Define or extract points pi(i=0, 1, 2, 3, …) to be matched on the reference image.

(2) For each point pi, determine its approximate height Zi and height error $\triangle$Zi. Zi and $\triangle$Zi can be predefined by users, or obtained by rough matching of high layer image pyramids or initial DSM. The quasi-epipolar lines of pi on the searching images are determined by known exterior parameters and line fitting methods. Define an image window W around pi, and W is named as correlation window.

(3) On one searching image's quasi-epipolar line, select a searching window (the same size as the correlation window) around each point of the line, compute the correlation coefficient between the searching window and correlation window, and find the local max correlation coefficients.

---

* Corresponding author. This is useful to know for communication with the appropriate person in cases with more than one author.
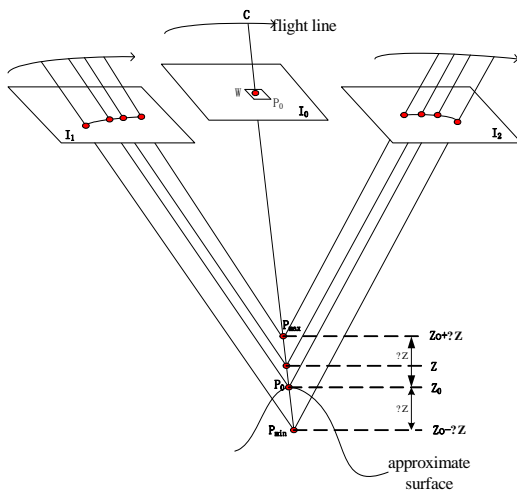
Figure1. Illustration of AMMGC model

(4) Check the local max correlation coefficients by another searching image to obtain one or zero candidate matching result (matching pixels).

(5) Compute the ground coordinates (Xi, Yi, Zi) of ground point Pi by forward intersection of the matching results.

3. PRECISE MODEL OF MULTIPLE IMAGES MATCHING

If we have obtained the image point in the reference image and its corresponding image point in searching image by AMMGC method , now how to use the least square matching of multiple images method to improve the results of initial mathching should be discussed in detail.

3.1 Gray Observation Equation

Suppose that   is an image patch (a rectangle or a square generally) whose center is   in the reference image, is an image patch whose center is   in the searching image and is the pixel coordinate. The reference image patch can be considered an observation of the searching image patch in the least squares adjustment. So the following observation equation can be established.

$$v_i(x, y) = T_r(g_i(T_g(x, y))) - g_0(x, y) \quad (i = 1, 2, ...n) \quad (1)$$

where g_0 = gray values of the reference image patch
   g_1 = gray values of the corresponding serching image patch

   (x,y) = pixe coordinates of image point
   $vi(x,y)$ = true error function
   T_r = radiation distortion of image
   T_g = geometric distortion of image

The radiation distortion can be solved when calculating the correlative coefficient, therefore the gray distortion between the reference image and the serching images do not be considered here .The equation (1) can be given by

$$v_i(x, y) = g_i(T_g(x, y)) - g_0(x, y) \quad (2)$$

The above equation is the least squares gray observation equation. Linearize the equation with regard to the pixel coordinate *(x,y)*and ignore the high-order terms, according to

$$v_i(x, y) = g_i(T_g(x_0, y_0)) + \frac{\partial g_i}{\partial x_i}\Delta x_i + \frac{\partial g_i}{\partial y_i}\Delta y_i - g_0(x, y) \quad (3)$$

Because of the very small field-of-view angle of an image patch, an affine transformation is considered to be satisfactory to model the geometric transformation between the grey values, with a reasonable assumption of a locally planar object surface.

$$T_g = \begin{cases} x_i = u_i + u_{xxi}x_0 + u_{xyi}y_0 \\ y_i = v_i + v_{yxi}x_0 + v_{yyi}y_0 \end{cases} (i = 1, 2, ...n) \quad (4)$$

The first order differentials of equation (4) can be expressed as

$$\begin{cases} \Delta x_i = \Delta u_i + x_0\Delta u_{xxi} + y_0\Delta u_{xyi} \\ \Delta y_i = \Delta v_i + x_0\Delta u_{yxi} + y_0\Delta u_{yyi} \end{cases} \quad (5)$$

with the simplified notation:

$$g_x^i = \frac{\partial g_i}{\partial x_i}; g_y^i = \frac{\partial g_i}{\partial y_i} \quad (6)$$

Combining equation (3) and equation (5) we obtain

$$v_i(x, y) = g_i(T_g(x_0, y_0)) + g_x^i\Delta u_i + g_x^i x_0\Delta u_{xxi} + g_x^i y_0\Delta u_{xyi} \quad (7)$$
$$+ \quad g_y^i\Delta v_i + g_y^i x_0\Delta v_{yxi} + g_y^i y_0\Delta u_{yyi} - g_0(x, y)$$

With the notations

$$\begin{cases} X_i^T = [\Delta u_i, \Delta u_{xxi}, \Delta u_{xyi}, \Delta v_i, \Delta v_{yxi}, \Delta v_{yyi}] \\ l_i = g_0(x, y) - g_i(T_g(x_0, y_0)) \quad (i = 1, 2, ...n) \\ A_i = [g_x^i, g_x^i x_0, g_x^i y_0, g_y^i, g_y^i x_0, g_y^i y_0] \end{cases}$$

$$X^T = [X_1^T, X_2^T, \cdots, X_n^T]; \quad l = [l_1, l_2, \cdots, l_n]; \quad A = \begin{bmatrix} A_1 & \cdots & 0 \\ \cdots & \cdots & \cdots \\ 0 & \cdots & A_n \end{bmatrix}$$

(8)

So the gray observation equation (1) can be expressed as

$$v(x, y) = AX - l; P \quad (\text{the weight coefficient matrix of } l)$$

(9)

3.2 The Geometrical Observation Equations

The qusi-epipolar line is used as constraint factor and maked up of the geometrical observation equations in this paper. As is shown in Figure 1, the corresponding point $p_i, i = 1, 2, ..., n(n \geq 2)$ in searching image must locate at their corresponding qusi-epipolar line, therefore these qusi-epipolar lines can be used as geometrical constraints and form corresponding geometrical observation equations to join the adjustment.Generally, the qusi-epipolar line can be expressed by the formation of polynomials

$$y_i = f(x_i) = a_{im} x_i^m + ... + a_{i1} x_i + a_{i0}$$

(10)

For the L0 level images of the linear array sensor, the qusi-epipolar lines are not the straight lines generally. But for the L1 level images, the qusi-epipolar line can be simulated by a straight line. Then Equation (10) becomes

$$y_i = f(x_i) = a_{i1} x_i + a_{i0}$$

(11)

If we have get the approximate pixel coordinate (x_i^0, y_i^0) of the image point by AMMGC, the geometrical observation equations can be expressed by

$$v(x, y) = \Delta y_i - a_{i1} \Delta x_i + (y_i^0 - f(x_i^0))$$

(12)

With the notations

$$\begin{cases} X_i^T = [\Delta x_i, \Delta y_i] \\ l_{gi} = -y_i^0 + f(x_i^0) \quad (i = 1, 2, ...n) \\ B_i = [-a_{i1}, 1] \end{cases}$$

$$X = [X_1^T, X_2^T, \cdots, X_n^T]^T; \quad l_g = [l_{g1}, l_{g2}, \cdots, l_{gi}]^T; \quad B = \begin{bmatrix} B_1 & \cdots & 0 \\ \cdots & \cdots & \cdots \\ 0 & \cdots & B_n \end{bmatrix}$$

(13)

Here $(\Delta x_i, \Delta y_i)$ is corresponding to $(\Delta u_i, \Delta v_i)$ gotten in the gray observation equations, so the geometrical observation equations can be given by

$$v(x, y) = BX - l_g; P_g \text{ (the weight coefficient matrix of } l_g)$$

(14)

Gray observation equations (9) and geometrical observation equations (14) compose a combined adjustment system, which are associated with each other via the common conversion parameter (u_i, v_i). The least square solution of combined adjustment is

$$\hat{X} = (A^T P A + B^T P_g B)^{-1} (A^T P l + B^T P_g l_g)$$

(15)

The answer of equation (15) is the final matching points coordinates, which can reach the 1/10 pixel matching accuracy in theory.

4. DSM GENERATION

Based on image pyramids and feature points, DSM are automated generated in this paper. Usually, feature points correspond to the points with acutely changing intensities, so they are fairly important for DSM generation. Additionally, feature points are precise and reliable, and they can be extracted by many methods.

However, in the image areas with coarse image textures and even no image textures, feature points can not be extracted. Therefore, apart from feature points, grid point has to be used to ensure the generation of precise and dense DSM. Grid points are the points evenly distributed among images. Compared with feature points, grid points may lie at image areas with coarse texture or even occluded and thus will obtain incorrect matching results.

On each image pyramid layer, matching results for feature points and grid points are obtained through multiple image matching algorithm. Feature points are matched through approximate DSM obtained from higher image pyramid layers and the matching results are used to constraint the searching distance of the grid points. In order to ensure the quality of the DSM, dense feature points and grid points have to be obtained in the matching process and the process is that as follows. Firstly, feature points with high interest values are extracted by Föerstne operator. Then, these points are matched by traditional 2D searching methods. Successful matching results are used to interpolate y-parallax gird, which are used to compensate the y-

parallax of the other points. Finally, along corresponding epipolar lines, the other points are searched and matched.

After the extraction of massive homogeneous points, these points' coordinates in the object space are computed through back-projection by known image orientation parameters and the original DSM can be generated.

5. EXPERIMENTS

Three ADS40 three-line-array digital images were used in this paper. These images ware obtained form the same flight strip. The main attributes of the images are shown in Table 1.

Camera	Level	Location	Focus	GSD	Flight height
ADS40	1	Lintong, China	62.7cm	0.48 m	1000 m

Table 1. Main attributes of experiment data

Using the multiple image matching algorithm model, three images are matched simultaneously, where the nadir image is used as reference image and the backward and forward images are used as searching images. During the matching process, for every feature points on the reference image, an initial height (provided by approximate DSM) is given and gradually changed by a certain step. The coordinates of the feature points in the object space are then computed and back-projected to get the points in searching images. Given a correlation window, correlation coefficients between reference image and searching images are computed. The relationship between height and correlation coefficients are plotted, and some are displayed in Figure 2 and Figure 3.
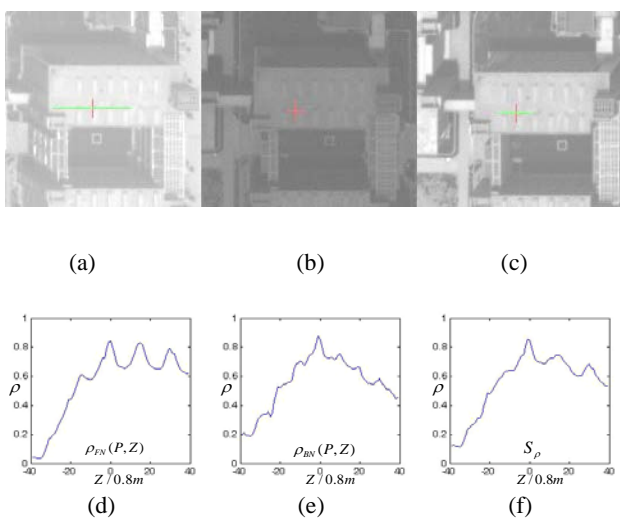

(a)   (b)   (c)

(d)   (e)   (f)

Figure2. Feature point matching results based on multi-image

In Figure 2，(a), (b), (c) is a part of forward, nadir and backward image respectively. The point marked by a red cross in the nadir image is feature point. The red line in the backward and forward image is the epipolar line and represents the searching distance. (d), (e), (f) is the correlation coefficients between forward and nadir image, the correlation coefficients

between backward and nadir image, and the mean coefficients of the above respectively. In (d), (e) and (f), the horizontal axis represents the height range, which changes 40 times with 0.8m step, and the vertical axis represents the correlation coefficients.
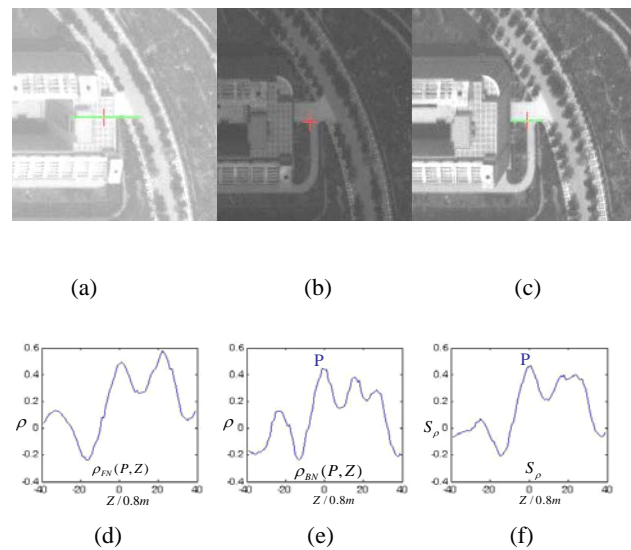

(a)   (b)   (c)

(d)   (e)   (f)

Figure3. Feature point matching results based on multi-image

In Figure 3，(a), (b), (c) is a part of forward, nadir and backward image respectively. The point marked by a red cross in the nadir image is feature point. The red line in the backward and forward image is the epipolar line and represents the searching distance. (d), (e), (f) is the correlation coefficients between forward and nadir image, the correlation coefficients between backward and nadir image, and the mean coefficients of the above respectively. In (d), (e) and (f), the horizontal axis represents the height range, which changes 40 times with 0.8m step, and the vertical axis represents the correlation coefficients. As can be seen from Fig 2(b), there are many similar features around the selected feature points. Traditional matching method based on two images can not obtain correct matching results, see Fig 2(d), (e), while based on the multiple image matching algorithm, correct matching results can be obtained, see figure 2(f). In Fig 3(a), the feature point is occluded in the forward image, and traditional matching method once again fails to find incorrect results (Fig 3(d)), while this problem can be avoided by the method proposed in this paper (Fig 3(f)).

Feature points and grid points (every 3 pixels of the reference image) are combined to generate dense points to match. On every image pyramid layer, these points are matched and used for the next image pyramid layer. After image matching, an initial DSM (Figure 4) can be generated from these points' coordinates obtained through back-projection. The DSM's quality has to be controlled. In our experiment, these points with or are reserved, while the other points (around 5%) are set as doubt points whose heights are interpolated by bilinear interpolation method. After some simple processing, the final DSM is shown in Figure 5.

6. CONCLUSIONS

From above, a new image matching algorithm model is proposed in this paper. This algorithm model can be used for aerial three line digital images and can match multiple images

simultaneously. The epipolar line constraints are also used indirectly in the model.
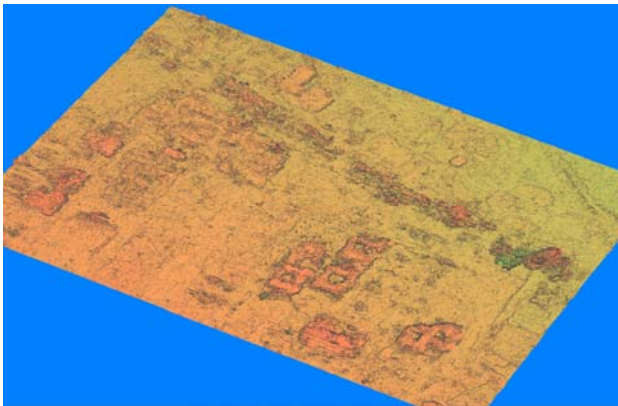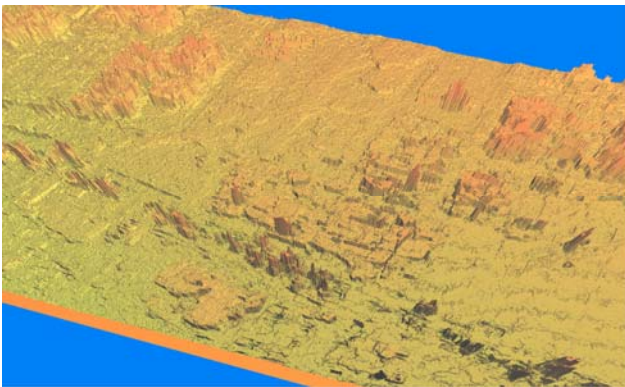

Figure 4 Initial DSM from matching points

Figure 5   Optimized DSM after quality control

From the experiments currently done, the algorithm shows great ability to improve matching reliability and can solve multiple

solution and occlusion problems effectively. Moreover, dense ground points and DSM can be generated through the combining of the algorithm model and some quality control measures.

However, massive ground points are not enough to generate precise DSM from high resolution images for urban areas. During the process of grid DSM interpolation, discontinuities are smoothed. This will lose a lot of information such as buildings' edge and make parts of DSM connected, which can be seen from Fig 4 and Fig 5. In order to generate more precise and practical DSM, edge features have to be extracted, matched and combined with point features in DSM generation, which will be our work in the future.

REFERENCES

X.H. Xiong, Y. Chen, and Z.B. Qian, A Fast, Accurate and Robust Image Matching Algorithm, Acta Geodaetica Cartographica Sinica, 2005, 34(1): pp. 40-44.

Y.S. Zhang, D.Z. Fan, and S. Ji, Multi-view Matching Algorithm Model for ADS40 Sensor, Journal of Zhengzhou Institute of Surveying and Mapping, 2007, 24(2): pp. 83-86.
Z.X. Zhang, From Digital Photogrammetry Workstation (DPW) to Digital Photogrammetry Grid (DPGird), Geomatics and Information Science of Wuhan University, 2007, 32(7): pp. 565-571.

Okutomi, M., Kanade, T. A Multiple-baseline Stereo. PAMI, 1993, Vol. 15, No. 4, pp. 53-363

Y.J. Zhang, Image Interpretation and Computer Vision, TSinghua University Press, Beijing, 1999. pp. 87-102.

D.Z. Fan. Theory and Algorithms of DSM Generation from Multi-line-array Images Matching, Institute of Surveying and Mapping for the degree of Doctor of Technical Sciences, 2007. pp. 35-57.